HHS Public Access

Author manuscript

Lupus. Author manuscript; available in PMC 2018 January 06.

Published in final edited form as:

Lupus. 2017 February ; 26(2): 170–178. doi:10.1177/0961203316657432.

Neuroimaging of Translocator Protein in Patients with Systemic Lupus Erythematosus: A Pilot Study Using [^{11}C]DPA-713 Positron Emission Tomography

Yuchuan Wang, PhD[1], **Jennifer M. Coughlin, MD**[2], **Shuangchao Ma**[1], **Christopher J. Endres, PhD**[1], **Michael Kassiou, PhD**[3], **Akira Sawa, MD, PhD**[2], **Robert F. Dannals, PhD**[1], **Michelle Petri, MD, MPH**[4], and **Martin G. Pomper, MD, PhD**[1,2]

[1]Russell H. Morgan Department of Radiology and Radiological Science, Johns Hopkins Medical Institutions, Baltimore, MD 21287

[2]Department of Psychiatry, Johns Hopkins Medical Institutions, Baltimore, MD 21287

[3]School of Chemistry, The University of Sidney, NSW 2006, Sydney, AU

[4]Department of Medicine, Johns Hopkins Medical Institutions, Baltimore, MD 21287

Abstract

Objective—Inflammation secondary to autoantibody-mediated effects occurring in multiple organs is a hallmark of systemic lupus erythematosus (SLE). The inflammatory response to SLE-mediated damage in brain parenchyma has been postulated in both normal and cognitively impaired individuals. Our goal is to use molecular imaging to investigate the distribution of the mitochondrial translocator protein (TSPO) within brain, which is upregulated during glial cell activation and considered as a marker of brain injury and repair.

Methods—We sought to characterize TSPO distribution in the brain of SLE patients using positron emission tomography (PET) and [^{11}C]DPA-713 (DPA), a radiopharmaceutical that targets TSPO. Eleven healthy controls and ten patients with SLE (years of diagnosis: 13.0 ± 7.7), all between the ages of 22 and 52, were imaged.

Results—Among the nine brain regions studied, no statistically significant increases in DPA binding were observed in SLE. Instead, there was a significant decrease in TSPO distribution in the cerebellum and hippocampus of SLE patients as compared to healthy controls. Such decreases were most significant in cognitively normal SLE subjects, but showed pseudo-normalization in those with cognitive impairment, due to higher cerebellar and hippocampal DPA binding in the cognitively impaired (as compared to normal) SLE brain.

Conclusion—Results from this pilot study suggest a link between diminished regional TSPO expression in the brain of patients with SLE, as well as possible glial cell activation within cerebellum and hippocampus of cognitively impaired individuals with SLE. Further studies are

Corresponding author: Martin G. Pomper, M.D., Ph.D., Johns Hopkins Medical School, 1550 Orleans St., 492 CRB II, Baltimore, MD 21287, Ph: 1-410-955-2789, Fax: 1-443-817-0990, mpomper@jhmi.edu.

DISCLOSURE

The authors have no potential conflict of interest relevant to this article.

needed to elucidate how mitochondrial dysfunction and glial cell activation may act together in SLE and SLE-mediated neurocognitive deficits.

Keywords

SLE; translocator protein (TSPO); glial cell activation; neurocognitive deficits; PET; molecular imaging

INTRODUCTION

Systemic lupus erythematosus (SLE) involves inflammation secondary to autoantibody-mediated effects on a variety of tissues as well as vasculopathy [1, 2]. Deposition of an immune complex may stimulate an innate immune response that leads to an increased release of pro-inflammatory cytokines and chemokines in the central nervous system (CNS). That cascade could have a role in the development of psychiatric symptoms, i.e., neuropsychiatric SLE (NPSLE) [2]. Autoantibody formation and immune complex deposition may result in cerebrovascular damage and vasculitis that permits passage of systemic inflammatory cells and pro-inflammatory cytokines across the blood-brain barrier and enter otherwise immune-privileged areas of the brain [3].

Hypermetabolic activity seen with positron emission tomography (PET) using ^{18}F-fluorodeoxyglucose (FDG) might serve as a visual signal of inflammation based on the increased metabolic demand of inflammatory cells, increased glucose transporter expression, and a cytokine-induced increase in the affinity of deoxyglucose for glucose transporters [1, 4, 5]. A study of 84 patients with newly diagnosed SLE (within nine months of initial diagnosis) reported hypermetabolism on FDG-PET in white matter regions, which correlated with systemic disease activity [1]. Further and more concrete evidence of change in regional brain immune and inflammatory responses in SLE may lead to better understanding of the underlying pathophysiology.

Activation of microglia, the innate immune cells of the brain, is considered an important component of brain immune and inflammatory responses. Microglial activation can be detected indirectly with radiopharmaceuticals targeting the translocator protein (TSPO) using PET [6]. TSPO, previously known as the peripheral benzodiazepine receptor (PBR), is a five-transmembrane protein that spans the outer mitochondrial membrane. While the physiological roles of TSPO are yet to be fully elucidated [7–9], upregulation of TSPO during microglial response to brain injury and repair has been noted [10]. That has provided an operating hypothesis for TSPO-targeting brain imaging studies. Mitochondrial dysfunction in T cells of patients with SLE has also been suggested [11, 12], and it is unknown whether similar dysfunction exists in microglia and can lead to diminished normal, physiological expression of TSPO. Both microglial and mitochondrial dysfunction are linked to neurologic and psychiatric disease [13–15].

TSPO-targeted PET radioligands have been used to study putative neuroinflammation in many diseases, e.g., [16–18]. Although widely used, the first generation of such radioligands, namely [^{11}C]*R*-PK11195, has demonstrated limited performance as a PET radiotracer [19]. A number of second-generation TSPO radiotracers, such as [^{11}C]DPA-713 (DPA),

[^{11}C]PBR28, and [^{18}F]FEPPA, have been developed and have shown improved brain delivery and increased specificity for TSPO [6, 19–21], which may, in turn, facilitate the study of various neurological diseases. For example, using [^{11}C]DPA-713 PET, we found that increased frontal cortex TSPO binding was specifically linked to HIV-associated dementia[22], while neuro-asymptomatic individuals infected with HIV demonstrated increases in other brain regions. In a recent study using [^{11}C]PBR28, it was shown that neuroinflammation, indicated by increased [^{11}C]PBR28 binding to TSPO in several brain regions (e.g., prefrontal cortex and hippocampus), occurs after conversion of mild cognitive impairment to Alzheimer's disease and worsens with disease progression [18].

Although a common single nucleotide polymorphism (SNP) in the *TSPO* gene (rs6971) has demonstrated deterministic effects on brain uptake of second generation TSPO PET radioligands [23], including DPA, these effects can be controlled during data analysis, as shown by [18 and 22]. The involvement of TSPO in the development of cutaneous pathology in a mouse model of SLE was previously studied [24], but to our knowledge no study of patients with SLE using TSPO-targeted brain PET has been reported.

Here we used a second-generation TSPO PET radiotracer, DPA, and an advanced high-resolution brain PET scanner, to conduct a pilot study of change in localized brain TSPO distribution in patients with SLE, and compared the data to that from age-matched, healthy controls. We chose to study a well-characterized group of patients in the later stages of SLE (more than 4 years of diagnosed disease), including individuals who were cognitively normal or impaired.

METHODS

Human Subjects

This study was approved by the Johns Hopkins Institutional Review Board and all subjects provided informed consent prior to participation. A total of 21 subjects under the age of 55 (healthy controls: N = 11; SLE: N = 10) underwent DPA PET neuroimaging. Healthy control subjects ranged in age from 22 to 52 years (mean ± standard deviation: 39.2 ± 11.1) and underwent a careful clinical interview to ensure health. None of the healthy participants had a history of medical disease or surgery during the previous year. They were not currently using prescribed or over-the-counter medications, with the exception of inclusion of one female participant taking an oral contraceptive. All healthy participants denied alcohol and illicit substance abuse, neurologic deficit, psychiatric illness, or head trauma with loss of consciousness.

Patients with a diagnosis of SLE were referred from the Johns Hopkins Rheumatology Clinic and a board-certified rheumatologist was on the study team (M.A.P.). All patients met revised ACR and SLICC classification criteria. These ten participants ranged in age from 23 to 51 years (41.1 ± 9.2) and the time since their diagnosis of SLE ranged from 4 to 29 years (13.0 ± 7.7). All SLE patients completed ANAM testing, among them, six subjects, who were all under the age of 49 (37.3 ± 8.8), were determined to have no cognitive impairment, while four (age: 36, 50, 50, and 51) were considered to be cognitively impaired, as each of the four individuals' performance was worse than one standard deviation below the mean

population performance on automated neuropsychological assessment metrics (ANAM) testing [25, 26]. The computerized assessment tests several neurocognitive domains and includes practice items before each test to ensure understanding and to standardize scores. It was administered over a 20 – 30 min period on a standard PC or laptop computer as we have previously reported [26, 27]. All subjects in both the SLE and control groups were also assessed for *TSPO* (rs6971) genotype as previously described [22].

Radiotracer Synthesis

Carbon-11 DPA-713 was synthesized by O-alkylation of its corresponding desmethyl phenolic precursor with [^{11}C]methyl triflate (from dry phase, high specific activity [^{11}C]methyl iodide) in acetone [28]. The radiotracer was purified by reverse phase HPLC and formulated by solid phase extraction as a sterile, apyrogenic solution of 14:1 0.9% saline:ethanol. The radiochemical purity at end of synthesis was >99% with an average specific activity of 850 ± 160 GBq per micromole (23000 ± 4400 mCi per micromole). The radiotracer product met all USP Chapter <823> acceptance criteria.

Brain Imaging

High specific activity [^{11}C]DPA-713 was delivered *via* an intravenous bolus injection at the onset of a 90 min dynamic list mode PET acquisition. The average injected dose was 688.1 (± 9.5) MBq. All participants underwent radial arterial line placement. The placement of an arterial line is necessary for obtaining the metabolite-corrected plasma input function, which is the standard practice for full quantitative analysis of PET radioligands with reversible binding characteristics in vivo. Measurement of the arterial plasma input function was conducted as previously described [19] through collection of 25 – 35 blood samples (1 mL) over the course of each 90 min PET scan. An additional eight serial 4 mL samples were collected for radiolabeled metabolite measurements.

PET scans were acquired using a second-generation High Resolution Research Tomograph (HRRT) scanner (Siemens Healthcare, Knoxville, TN), an LSO-based, dedicated brain PET system with 2.5 mm resolution [29]. The 90 min list mode data were binned into 30 frames (four 15 s, four 30 s, three 1 min, two 2 min, five 4 min, and twelve 5 min frames). The data were then reconstructed using the iterative ordered subset expectation maximization (OS-EM) algorithm (with six iterations and 16 subsets), with correction for radioactive decay, dead time, attenuation, scatter and randoms [30]. The attenuation maps were generated from 6 min transmission scans performed with a ^{137}Cs point source prior to the emission scans. The reconstructed image space consisted of cubic voxels, each 1.22 mm^3 in size, and spanning dimensions of 31 cm × 31 cm (transaxially) and 25 cm (axially).

All subjects also underwent brain magnetic resonance (MR) imaging to facilitate anatomical delineation of regions of interest (ROIs) on brain PET images after PET-MR co-registration (detailed below). MR T1-weighted images were obtained on either a 1.5T Signa Advantage system (GE Medical Systems, Waukesha, WI) as previously described [19] or on a Phillips Achieva 3T scanner (Andover, MA) with a 32-channel head coil to obtain a 1 × 1 × 1 mm 3D MP-RAGE sequence.

Data Analysis

The software package PMOD (v3.3, PMOD Technologies Ltd, Zurich, Switzerland) was used in the initial PET image processing and kinetic analysis. The steps included: (1) inter-frame motion correction: all 30 frames of PET-reconstructed images were rigidly realigned to the 0 – 30 min mean PET image, which was obtained by averaging frames 1 through 18; and, (2) PET-MR co-registration: the 0 – 30 min PET mean image and, subsequently, all 30 motion-corrected PET frames, were co-registered to the subject's T1-weighted MR image using rigid transformations. Based on the T1-weighted MR images, automated cortical reconstruction and volumetric segmentation were performed with the Freesurfer image analysis suite, which is freely available online (http://surfer.nmr.mgh.harvard.edu/). Technical details of those procedures are described in prior publications, e.g., [31].

Based on the affected brain regions indicated in the SLE literature, e.g., [1, 32–36], we generated nine ROIs, including cerebellum, hippocampus, amygdala, three white matter regions (frontal, parietal, and occipital), and three cortical gray matter regions (frontal, parietal, and occipital), by combining the corresponding sub-regions provided by Freesurfer. An ROI containing the entire cortical gray matter (GM) region was also defined to serve as a covariate or normalization factor in the subsequent statistical analysis, as discussed in previous PET studies using [^{11}C]*R*-PK-11195 [16] and DPA [22]. PET time-activity curves (TACs) were generated for all subjects using the above ROI definitions. Based on the TACs obtained, DPA binding to TSPO was quantified with the use of the metabolite-corrected arterial plasma input function. Following the published studies of ours and others using second-generation TSPO radioligands and the proposed nomenclature for reversibly binding radioligands [37], the total distribution volume (V_T) for each brain region was obtained using the Logan graphical method (t*=30 min), which represents the ratio of the radioligand concentration in brain tissue to that in plasma at equilibrium, which is proportional to the receptor density in the defined ROI.

Statistical analyses were performed with multivariate general linear modeling (GLM) of the V_T data using SPSS Statistics (Version 22.0, IBM Corp., Armonk, NY) so that the effects of several factors could be examined. Specifically, we modeled the V_T values obtained above from the nine selected ROIs based on their relationship to between-subject factors, including four independent fixed factors and two covariates. The fixed factors were cohort (SLE or control), TSPO genotype (C/C: high affinity binder, or, C/T: mixed affinity binder), gender (male or female), and cognitive status (normal or impaired). The covariates were the individual subject's age [38–40] and radiotracer binding in his/her entire cortical gray matter [16, 22]. Based on hypothesized change in regional TSPO distribution with SLE as well as with the onset of cognitive impairment, our main interest was to investigate the between-subject effects of cohort and cognitive status.

As an alternative method of analysis, we also performed an independent sample non-parametric (Wilcoxon-Mann-Whitney) test, comparing gray matter normalized V_T values ($_{GM}V_T$) between the sub-cohorts of patients (cognitively normal vs. impaired) and the corresponding age-matched cohort of healthy control individuals. The use of $_{GM}V_T$ has been shown to be an effective empirical approach [22] for eliminating genotypic differences while improving the consistency of the data (including intra-subject reproducibility and inter-

subject agreement among healthy controls). The threshold for significance in all statistical tests was set as $P < 0.005$, by taking into account multiple comparisons for the nine ROIs using the Bonferroni correction ($0.05/9 \approx 0.0056$).

RESULTS

Among eleven control subjects assessed for the rs6971 polymorphism, eight were found to have the C/C genotype and three with the C/T genotype. For the ten SLE subjects, five had the C/C genotype and five had the C/T genotype. Analysis of the MR images through quantitative evaluation of the segmentation results obtained with FreeSurfer showed no evidence of regional brain atrophy in SLE in any regions studied, including cerebellum, hippocampus, amygdala, three white matter regions (frontal, parietal, and occipital), and three cortical gray matter regions (frontal, parietal, and occipital). Subject demographics, in the form of between-subject factors from all 21 subjects, including the GM V_T obtained from PET imaging, are listed in Table 1. Based on the between-subject factors (Table 1), the GLM multivariate procedure was carried out for analyzing regional V_T data (in 9 brain regions) from the PET studies. Using full factorial modeling, the tests of between-subject factors revealed that the fixed factor: cohort (SLE vs. normal) led to effects at $P < 0.05$ in only two brain regions: cerebellum and hippocampus. The presence of cognitive impairment ("COGIMP" factor) had effects in the same two regions at $P < 0.05$, but not within the other regions. The complete statistical "F" and "Sig" (*P*-value) results from GLM multivariate analysis of all regions are listed in Table 2 for these two fixed factors. With Bonferroni correction, a significant difference ($P < 0.005$) between SLE and control cohorts was still present in the cerebellum, with SLE showing lower binding than controls as detailed in Table 3.

Table 3 depicts the estimated marginal means of V_T, obtained during the GLM multivariate analysis, to quantify the above mentioned effects. As shown, the cohort of patients with SLE had lower mean binding of DPA (mean regional V_T) than controls in both cerebellum and hippocampus. Within patients with SLE, the cognitively impaired individuals showed higher radiotracer binding (mean regional V_T) than cognitively normal patients, effectively leading to a "pseudo-normalization." In Figure 1 we show the estimated marginal means of V_T for these two regions to demonstrate such a pseudo-normalization, going from cognitively normal to impaired in SLE, when compared to controls. Such pseudo-normalization was absent in other regions analyzed (with frontal cortex shown as an example in Figure 1).

The results of non-parametric tests of independent samples (GM normalized distribution volume ${}_{GM}V_T$ in all ROIs) showed similar findings. In Figure 2 we plotted the individual ${}_{GM}V_T$ values in three representative brain regions: cerebellum, hippocampus, and frontal cortex. The individual data points for SLE subjects were grouped as cognitively normal (N = 6) and impaired (N = 4). The data points for the younger control subjects (age < 50, N = 8) were plotted separately to match better the age of the cognitively normal SLE subgroup, as there have been inconsistent reports on how aging may affect TSPO [38–40].

There was a trend toward lower radiotracer binding in cerebellum and hippocampus for the sub-group of patients without cognitive impairment, when compared to the age-matched

control subgroup (see Figure 2 legend for age comparison). Increased radiotracer binding in those two regions was seen in the cognitively impaired (and older) SLE individuals when compared to normal (and younger) SLE patients, whereas the opposite trend was suggested when comparing the younger and older healthy controls, who were all cognitively normal. The observations were unique to cerebellum and hippocampus, and were not significant in other regions, such as frontal cortex, as shown in Figure 2. The significance of the differences obtained using the non-parametric test was shown as *P*-values in Figure 2. With the threshold established by Bonferroni correction, a significant difference ($P < 0.005$) was found in cerebellum between the cognitively normal SLE sub-cohort and age-matched control sub-group. In Figure 3, representative PET parametric images depict the findings.

DISCUSSION

Results from this pilot study of 21 subjects (11 healthy controls and 10 SLE patients) suggest that patients with SLE may have lower cerebellar TSPO expression, as suggested by diminished binding of DPA. Interestingly, those patients without cognitive impairment reveal the most significant decrease in binding to TSPO in this region compared to age-matched healthy controls. The three elderly patients with cognitive impairment showed a trend toward increased binding, which the normal SLE patients did not, effectively leading to pseudo-normalization in this same region. The findings underline the importance of continued study of the possible role of increased TSPO expression, indicative of glial cell activation, in the pathophysiology of SLE-related cognitive impairment.

While the observed lower TSPO expression in cognitively normal SLE appeared to be paradoxical with our operating hypothesis, we note that the scientific community's understanding about TSPO is incomplete and still evolving. Although it has been observed many years ago that TSPO overexpression coincides with microglia activation in various pathological conditions – the initial hypothesis for this and many other previous TSPO imaging studies – to date, researchers still have not been able to convincingly connect such observations to mechanistic explanations. On the other hand, decreased TSPO expressions were found in neutrophils of X-linked chronic granulomatous disease patients, which may be linked to impaired superoxide production and bactericidal activity in this inherited phagocyte disease characterized by a deficiency in gp91phox [41]. Diminished TSPO expression has also recently been shown to result in altered oxygen metabolism and reduced ATP production in TSPO murine knockout models [7]. Published reports also supported key roles of imbalanced production and neutralization of reactive oxygen species and underlying disruption in mitochondrial homeostasis in SLE, e.g., [11, 12]. Further studies are needed to investigate how pathways of oxidative pathogenesis in SLE may be linked to diminished expression of mitochondrial TSPO in susceptible brain regions, for example, by combining TSPO-targeted PET imaging with assay of peripheral or central markers of oxidative stress over the longitudinal course of SLE. The "paradoxical" findings observed by us in this study may indicate that it is entirely possible that, under certain pathological conditions, while neuroinflammation might exist, TSPO expressions are unchanged or even diminished. Such observations are important catalysts for future studies to seek mechanistic insights for TSPO, microglia activation, and neuroinflammation.

Abnormality in cerebellum was a major finding in a recently published resting-state functional MR study of SLE patients without neuropsychiatric complications [35]. In our pilot study, the finding of diminished TSPO distribution in the cerebellums of cognitively normal SLE subjects not only survived Bonferroni correction, but also had an observed power of 95.4% through GLM multivariate analysis, despite the small sample size.

One may seek to explain the lower cerebellar TSPO binding in cognitively normal SLE subjects by degradation of tissue and apoptosis, which were thought to be responsible for regional brain hypometabolism (abnormally low glucose utilization) observed in both early-stage and late-stage SLE cohorts in previous studies [1, 32, 34]. However, hypometabolism was found only in the frontal and parietal cortices, but not in the cerebellum. Combining those results and two observations from our study, (a) no cerebellar atrophy in the SLE cohort was observed based on MR, and (b) cognitively impaired SLE patients exhibited TSPO pseudo-normalization of the cerebellum on DPA PET (as shown by Figures 1–3), it may be plausible to link the diminishing cerebellar TSPO in SLE to mitochondrial dysfunction.

Although regional hypermetabolism, an indirect indicator of neuroinflammation, was reported previously in a cohort of newly diagnosed SLE patients [1], we did not observe SLE-mediated TSPO upregulation in this study, where all participating SLE patients were at least four years out from initial diagnosis. We cannot exclude the possibility that increased exposure to immune and disease-modifying medications over the longer duration of illness in our cohort may contribute to such observations. However, the trend of increased DPA binding in cerebellum of more elderly, cognitively impaired patients with SLE, in spite of a long duration of treatment, suggests a more complex role for TSPO expression as well as glial cell activation, over the course of SLE. The combined effects of glial cell activation and SLE-related mitochondrial dysfunction may have resulted in the observed pseudo-normalization. We previously demonstrated a similar pseudo-normalization phenomenon in several brain regions in a neuroimaging study of serotonergic transmission in HIV with [^{11}C]DASB-PET [42], which was thought result from the combined effects of HIV-associated neurodegeneration and depression-associated dysregulation of serotonergic transmission.

CONCLUSIONS

Our results suggest that altered TSPO distribution in the cerebellum, and potentially in other regions (e.g., hippocampus), may be a marker of pathophysiology in in SLE. Studies are under way to provide direct evidence on whether the changes demonstrated are linked to mitochondrial dysfunction, and how such dysfunction may affect SLE brain. Building upon such evidence and future TSPO-targeted PET imaging of more patients with SLE, both with and without cognitive impairment, the cerebellar pseudo-normalization observed in this pilot study may be further substantiated, providing clues connecting regional glial cell activation and SLE-mediated neuropsychiatric symptoms.

Acknowledgments

The authors thank the Lupus Foundation of America, NIH MH082277, and NIH AR43727 for financial support, Judy Buchanan for editing the manuscript and the Johns Hopkins PET Center for expert provision of [^{11}C]DPA-713.

Financial Support

Grants from Lupus Foundation of America (MGP), NIH MH082277 (CJE), and NIH AR43727 (MP)

References

1. Ramage AE, et al. Neuroimaging evidence of white matter inflammation in newly diagnosed systemic lupus erythematosus. Arthritis Rheum. 2011; 63:3048–57. [PubMed: 21618460]
2. Santer DM, Yoshio T, Minota S, Moller T, Elkon KB. Potent induction of IFN-alpha and chemokines by autoantibodies in the cerebrospinal fluid of patients with neuropsychiatric lupus. J Immunol. 2009; 182:1192–201. [PubMed: 19124763]
3. Brooks WM, et al. The histopathologic associates of neurometabolite abnormalities in fatal neuropsychiatric systemic lupus erythematosus. Arthritis Rheum. 2010; 62:2055–63. [PubMed: 20309864]
4. Curiel R, Akin EA, Beaulieu G, DePalma L, Hashefi M. PET/CT imaging in systemic lupus erythematosus. Ann N Y Acad Sci. 2011; 1228:71–80. [PubMed: 21718325]
5. Jamar F, et al. EANM/SNMMI guideline for 18F-FDG use in inflammation and infection. J Nucl Med. 2013; 54:647–58. [PubMed: 23359660]
6. Chauveau F, Boutin H, Van Camp N, Dolle F, Tavitian B. Nuclear imaging of neuroinflammation: a comprehensive review of [11C]PK11195 challengers. Eur J Nucl Med Mol Imaging. 2008; 35:2304–19. [PubMed: 18828015]
7. Banati RB, et al. Positron emission tomography and functional characterization of a complete PBR/TSPO knockout. Nat Commun. 2014; 5:5452. [PubMed: 25406832]
8. Fan J, Campioli E, Midzak A, Culty M, Papadopoulos V. Conditional steroidogenic cell-targeted deletion of TSPO unveils a crucial role in viability and hormone-dependent steroid formation. Proc Natl Acad Sci U S A. 2015; 112:7261–6. [PubMed: 26039990]
9. Selvaraj V, Stocco DM. The changing landscape in translocator protein (TSPO) function. Trends Endocrinol Metab. 2015
10. Chen MK, Guilarte TR. Translocator protein 18 kDa (TSPO): molecular sensor of brain injury and repair. Pharmacol Ther. 2008; 118:1–17. [PubMed: 18374421]
11. Perl A. Oxidative stress in the pathology and treatment of systemic lupus erythematosus. Nat Rev Rheumatol. 2013; 9:674–86. [PubMed: 24100461]
12. Perl A, Gergely P Jr, Banki K. Mitochondrial dysfunction in T cells of patients with systemic lupus erythematosus. Int Rev Immunol. 2004; 23:293–313. [PubMed: 15204090]
13. Aguzzi A, Barres BA, Bennett ML. Microglia: scapegoat, saboteur, or something else? Science. 2013; 339:156–61. [PubMed: 23307732]
14. Manji H, et al. Impaired mitochondrial function in psychiatric disorders. Nat Rev Neurosci. 2012; 13:293–307. [PubMed: 22510887]
15. Stephan BC, et al. The neuropathological profile of mild cognitive impairment (MCI): a systematic review. Mol Psychiatry. 2012; 17:1056–76. [PubMed: 22143004]
16. Doorduin J, et al. Neuroinflammation in schizophrenia-related psychosis: a PET study. J Nucl Med. 2009; 50:1801–7. [PubMed: 19837763]
17. Venneti S, Lopresti BJ, Wiley CA. The peripheral benzodiazepine receptor (Translocator protein 18kDa) in microglia: from pathology to imaging. Prog Neurobiol. 2006; 80:308–22. [PubMed: 17156911]
18. Kreisl WC, et al. In vivo radioligand binding to translocator protein correlates with severity of Alzheimer's disease. Brain. 2013; 136:2228–38. [PubMed: 23775979]
19. Endres CJ, et al. Initial evaluation of 11C-DPA-713, a novel TSPO PET ligand, in humans. J Nucl Med. 2009; 50:1276–82. [PubMed: 19617321]
20. Brown AK, et al. Radiation dosimetry and biodistribution in monkey and man of 11C-PBR28: a PET radioligand to image inflammation. J Nucl Med. 2007; 48:2072–9. [PubMed: 18006619]
21. Rusjan PM, et al. Quantitation of translocator protein binding in human brain with the novel radioligand [18F]-FEPPA and positron emission tomography. J Cereb Blood Flow Metab. 2011; 31:1807–16. [PubMed: 21522163]

22. Coughlin JM, et al. Regional brain distribution of translocator protein using [11C]DPA-713 PET in individuals infected with HIV. J Neurovirol. 2014
23. Owen DR, et al. An 18-kDa translocator protein (TSPO) polymorphism explains differences in binding affinity of the PET radioligand PBR28. J Cereb Blood Flow Metab. 2012; 32:1–5. [PubMed: 22008728]
24. Bribes E, Galiegue S, Bourrie B, Casellas P. Involvement of the peripheral benzodiazepine receptor in the development of cutaneous pathology in Mrl/Lpr mice. Immunol Lett. 2003; 85:13–8. [PubMed: 12505191]
25. Reeves, D. User's manual: Clinical and neurotoxicology subset. National Cognitive Foundation; San Diego, CA: 1996. Automated neuropsychological assessment metrics (ANAM V3.11a/96). (Report No. NCRF-SR-96-01)
26. Petri M, et al. Depression and cognitive impairment in newly diagnosed systemic lupus erythematosus. J Rheumatol. 2010; 37:2032–8. [PubMed: 20634244]
27. Fangtham M, Petri M. 2013 update: Hopkins lupus cohort. Curr Rheumatol Rep. 2013; 15:360. [PubMed: 23888367]
28. Thominiaux C, et al. Improved synthesis of the peripheral benzodiazepine receptor ligand [11C]DPA-713 using [11C]methyl triflate. Appl Radiat Isot. 2006; 64:570–3. [PubMed: 16427784]
29. Wienhard K, et al. The ECAT HRRT: performance and first clinical application of the new high resolution research tomograph. Nuclear Science, IEEE Transactions on. 2002; 49:104–110.
30. Rahmim A, et al. Statistical list-mode image reconstruction for the high resolution research tomograph. Phys Med Biol. 2004; 49:4239–58. [PubMed: 15509063]
31. Fischl B, et al. Whole brain segmentation: automated labeling of neuroanatomical structures in the human brain. Neuron. 2002; 33:341–55. [PubMed: 11832223]
32. Zardi EM, Taccone A, Marigliano B, Margiotta DP, Afeltra A. Neuropsychiatric Systemic Lupus Erythematosus: Tools for the diagnosis. Autoimmun Rev. 2014
33. Watson P, Storbeck J, Mattis P, Mackay M. Cognitive and emotional abnormalities in systemic lupus erythematosus: evidence for amygdala dysfunction. Neuropsychol Rev. 2012; 22:252–70. [PubMed: 22886588]
34. Lee SW, Park MC, Lee SK, Park YB. The efficacy of brain (18)F-fluorodeoxyglucose positron emission tomography in neuropsychiatric lupus patients with normal brain magnetic resonance imaging findings. Lupus. 2012; 21:1531–7. [PubMed: 22941565]
35. Lin Y, et al. Localization of cerebral functional deficits in patients with non-neuropsychiatric systemic lupus erythematosus. Hum Brain Mapp. 2011; 32:1847–55. [PubMed: 21170956]
36. Muscal E, Brey RL. Neurologic manifestations of systemic lupus erythematosus in children and adults. Neurol Clin. 2010; 28:61–73. [PubMed: 19932376]
37. Innis RB, et al. Consensus nomenclature for in vivo imaging of reversibly binding radioligands. J Cereb Blood Flow Metab. 2007; 27:1533–9. [PubMed: 17519979]
38. Gulyas B, et al. Age and disease related changes in the translocator protein (TSPO) system in the human brain: positron emission tomography measurements with [11C]vinpocetine. Neuroimage. 2011; 56:1111–21. [PubMed: 21320609]
39. Kumar A, et al. Evaluation of age-related changes in translocator protein (TSPO) in human brain using (11)C-[R]-PK11195 PET. J Neuroinflammation. 2012; 9:232. [PubMed: 23035793]
40. Suridjan I, et al. Neuroinflammation in healthy aging: a PET study using a novel Translocator Protein 18kDa (TSPO) radioligand, [(18)F]-FEPPA. Neuroimage. 2014; 84:868–75. [PubMed: 24064066]
41. Zavala F, Veber F, Descamps-Latscha B. Altered expression of neutrophil peripheral benzodiazepine receptor in X-linked chronic granulomatous disease. Blood. 1990; 76:184–8. [PubMed: 2163694]
42. Hammoud DA, et al. Imaging serotonergic transmission with [11C]DASB-PET in depressed and non-depressed patients infected with HIV. Neuroimage. 2010; 49:2588–95. [PubMed: 19853044]

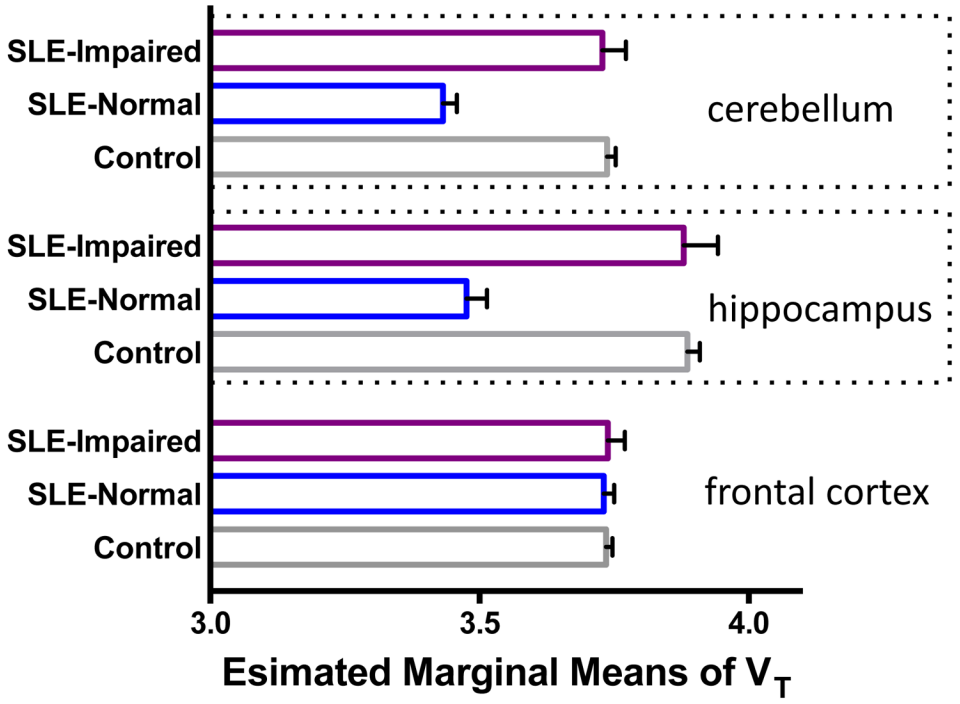

Figure 1.

Comparison of estimated marginal means of V_T in cerebellum, hippocampus, and frontal cortex, obtained during the GLM multivariate analysis. Within patients with SLE, the cognitively impaired individuals (N = 4) showed higher radiotracer binding (mean regional V_T) than cognitively normal patients with SLE (N = 6). Cognitively normal patients with SLE had diminished DPA binding compared to controls (N = 11). A pseudo-normalization was observed, going from cognitively normal to impaired in SLE, when compared to controls. Covariates appearing in the model are evaluated at the following values: V_{T_GM} = 3.689, Age = 40.095.

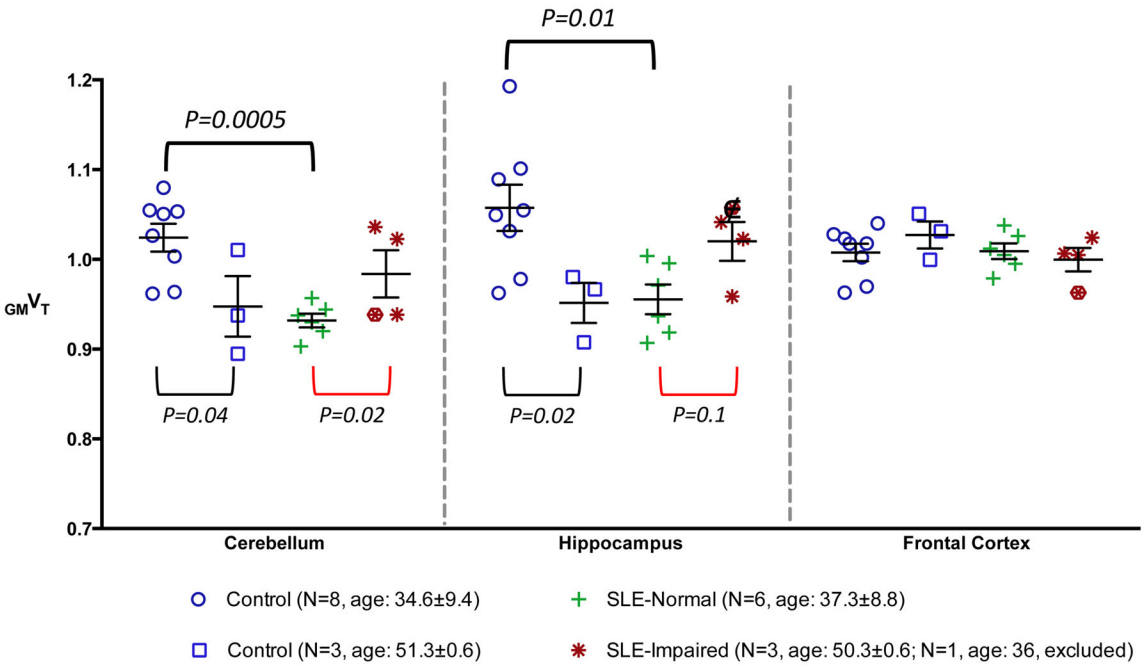

Figure 2.

Plots of individual gray matter normalized distribution volume ($_{GM}V_T$) in three representative brain regions: cerebellum, hippocampus, and frontal cortex. The individual data points for SLE subjects were grouped as cognitively normal and impaired. For control subjects, younger (age < 50) and older subjects were grouped separately to match better the age of two SLE subgroups. The significance of these differences obtained using the non-parametric test was shown as *P*-values. Data from the 36-year-old cognitively impaired SLE subject, designated with "□" was excluded from non-parametric testing due to age mismatch with other impaired SLE subjects.

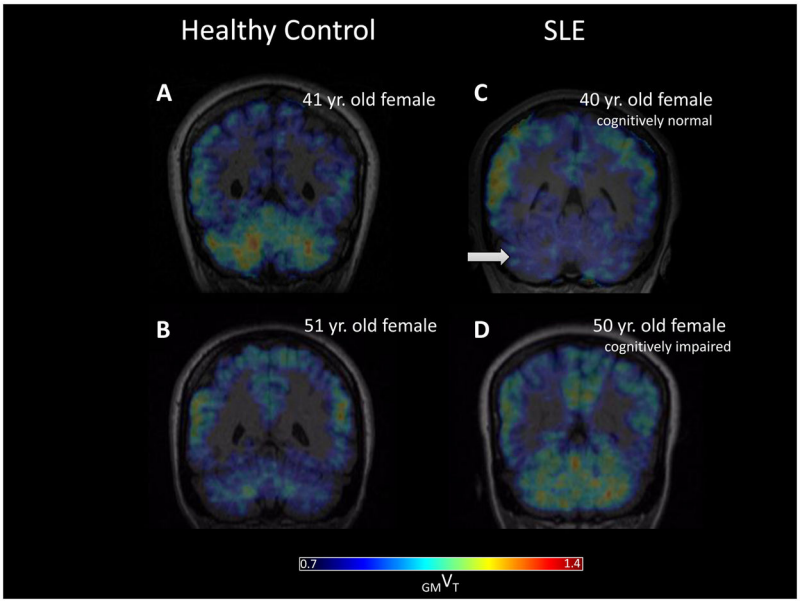

Figure 3.

Representative coronal view of DPA PET parametric ($_{GM}V_T$) images from age-matched control (**A**, **B**) and SLE (**C**, **D**) subjects. The cognitively normal SLE patient showed lower radiotracer binding in cerebellum (arrow in **C**) than the healthy control subject. Increased radiotracer binding in cerebellum was seen in the older, cognitively impaired SLE patient (**B**) when compared to **C**, whereas the opposite trend was suggested when comparing the younger (**A**) and older (**B**) healthy controls.

Lupus. Author manuscript; available in PMC 2018 January 06.

Table 1

Summary of between-subjects factors. The fixed factors are cohort (control or SLE), genotype (C/C or C/T), gender (M: male or F: female), and COGIMP (N: cognitively normal, Y: impaired). The covariates were an individual subject's age and radiotracer binding in his/her entire cortical gray matter (V_{T_GM}).

Subject No.	Cohort	Genotype	Gender	COGIMP	Age	V_{T_GM}
1	Control	C/C	M	N	22	6.04
2	Control	C/C	M	N	23	3.82
4	Control	C/C	M	N	45	3.17
3	Control	C/C	F	N	32	5.05
5	Control	C/C	F	N	36	3.96
6	Control	C/C	F	N	47	3.13
7	Control	C/C	F	N	51	5.15
8	Control	C/C	F	N	51	3.98
9	Control	C/T	M	N	31	1.64
10	Control	C/T	M	N	52	1.66
11	Control	C/T	F	N	41	2.73
12	SLE	C/C	M	N	43	3.14
13	SLE	C/C	F	N	23	3.96
14	SLE	C/C	F	N	32	3.87
15	SLE	C/C	F	N	38	6.97
16	SLE	C/C	F	Y	50	4.33
17	SLE	C/T	F	N	40	2.71
18	SLE	C/T	F	N	48	4.33
19	SLE	C/T	F	Y	36	3.04
20	SLE	C/T	F	Y	50	2.71
21	SLE	C/T	F	Y	51	2.07

Table 2

Result from tests of between-subjects factors using the GLM multivariate procedure. The statistical “F” and “Sig.” (*P*-value) results from GLM multivariate analysis of all regions are listed for two of the fixed factors: cohort and COGIMP. With Bonferroni correction, a significant difference ($P < 0.005$) between SLE and control cohorts was present in the cerebellum.

Region	Cohort (Control vs. SLE)		COGIMP (Normal vs. Impaired)	
	F	Sig. (*P*)	F	Sig. (*P*)
Cerebellum	16.454	.002**	8.175	.017*
Hippocampus	8.950	.014*	7.423	.021*
Amygdala	2.188	.170	.917	.361
Occipital cortex	1.049	.330	.173	.686
Occipital white matter	1.335	.275	.649	.439
Frontal cortex	.006	.940	.139	.717
Frontal white matter	.172	.687	.114	.743
Parietal cortex	3.577	.088	.292	.601
Parietal white matter	.114	.743	.547	.476

*$P < 0.05$

**$P < 0.005$

Table 3

Estimated marginal means of V_T comparing the effect of cohort (control vs. SLE), as well as the effect of cognitive status (normal vs. impaired), in cerebellum and hippocampus. These effects showed $P < 0.05$ significance in GLM multivariate analysis (Table 2).

				95% Confidence Interval	
Region	**Cohort**	**Mean**	**Std. Error**	**Lower Bound**	**Upper Bound**
Cerebellum	Control	3.737[a,b]	.052	3.620	3.854
	SLE	3.550[a,b]	.051	3.437	3.663
Hippocampus	Control	3.886[a,b]	.077	3.714	4.058
	SLE	3.637[a,b]	.075	3.471	3.804
	Cognitive Status				
Cerebellum	Normal	3.606[a,b]	.040	3.517	3.695
	Impaired	3.728[a,b]	.087	3.535	3.921
Hippocampus	Normal	3.711[a,b]	.059	3.580	3.841
	Impaired	3.879[a,b]	.127	3.595	4.163

[a] Covariates appearing in the model are evaluated at the following values: $V_{T\_GM} = 3.689$, $Age = 40.095$.

[b] Based on modified population marginal mean.